

# Suppression of Cytokine-Mediated Complement Factor Gene Expression through Selective Activation of the Ah Receptor with 3',4'-Dimethoxy- $\alpha$ -naphthoflavone<sup>[S]</sup>

Iain A. Murray, Colin A. Flaveny, Christopher R. Chiaro, Arun K. Sharma, Rachel S. Tanos, Jennifer C. Schroeder, Shantu G. Amin, William H. Bisson, Siva K. Kolluri, and Gary H. Perdew

Center for Molecular Toxicology & Carcinogenesis, Department of Veterinary & Biomedical Sciences, the Pennsylvania State University, University Park, Pennsylvania (I.A.M., C.A.F., C.R.C., R.S.T., J.C.S., G.H.P.); Department of Pharmacology, Milton S. Hershey Medical Center, the Pennsylvania State University, Hershey, Pennsylvania (A.K.S., S.G.A.); Cancer Biology Laboratory, Department of Environmental and Molecular Toxicology, Environmental Health Sciences Center, Oregon State University, Corvallis, Oregon (W.H.B., S.K.K.) and Pharmaceutical Biochemistry Group, School of Pharmaceutical Sciences, University of Geneva, Geneva, Switzerland (W.H.B.)

Received October 12, 2010; accepted December 1, 2010

## ABSTRACT

We have characterized previously a class of aryl hydrocarbon receptor (AHR) ligand termed selective AHR modulators (SAhRMs). SAhRMs exhibit anti-inflammatory properties, including suppression of cytokine-mediated acute phase genes (e.g., *Saa1*), through dissociation of non-dioxin-response element (DRE) AHR activity from DRE-dependent xenobiotic gene expression. The partial AHR agonist  $\alpha$ -naphthoflavone ( $\alpha$ NF) mediates the suppressive, non-DRE dependent effects on *SAA1* expression and partial DRE-mediated *CYP1A1* induction. These observations suggest that  $\alpha$ NF may be structurally modified to a derivative exhibiting only SAhRM activity. A screen of  $\alpha$ NF derivatives identifies 3',4'-dimethoxy- $\alpha$ NF (DiMNF) as a candidate SAhRM. Competitive ligand binding validates DiMNF as an AHR ligand, and DRE-dependent reporter assays with quantitative mRNA analysis of AHR target genes reveal minimal agonist activity associated with AHR binding. Consistent with loss of agonist activity,

DiMNF fails to promote AHR binding to DRE probes as determined through electromobility shift assay. Importantly, mRNA analysis indicates that DiMNF retains the suppressive capacity of  $\alpha$ NF regarding cytokine-mediated *SAA1* expression in Huh7 cells. Interestingly, predictive docking modeling suggests that DiMNF adopts a unique orientation within the AHR ligand binding pocket relative to  $\alpha$ NF and may facilitate the rational design of additional SAhRMs. Microarray studies with a non-DRE binding but otherwise functional AHR mutant identified complement factor C3 as a potential SAhRM target. We confirmed this observation in Huh7 cells using 10  $\mu$ M DiMNF, which significantly repressed C3 mRNA and protein. These data expand the classes of AHR ligands exerting DRE-independent anti-inflammatory SAhRM activity, suggesting SAhRMs may have application in the amelioration of inflammatory disorders.

## Introduction

The acute-phase response (APR) represents an adaptive response that occurs upon exposure to a variety of stimuli, including infection, burn injury, trauma, and chronic inflam-

matory diseases (Kushner and Rzewnicki, 1994). The release of cytokines into circulation activates the APR in the liver, leading to dramatic change in the expression and secretion of a wide variety of acute phase proteins (APPs). Proteins classified as an APP include C-reactive protein, serum amyloid A (SAA), haptoglobin,  $\alpha$ 1-antitrypsin, and complement C3. These proteins in turn help the organism respond to the stress through a number of mechanisms. However, persistent inflammatory disease states, such as cancer or autoimmune disease (e.g., Crohn's disease, multiple sclerosis, rheumatoid arthritis), can lead to APP actually participating in inflam-

This work was supported by the National Institutes of Health National Institute of Environmental Health Sciences [Grant ES04869].

Article, publication date, and citation information can be found at <http://molpharm.aspetjournals.org>.  
doi:10.1124/mol.110.069369.

[S] The online version of this article (available at <http://molpharm.aspetjournals.org>) contains supplemental material.

**ABBREVIATIONS:** APR, acute-phase response; AHR, aryl hydrocarbon receptor; APP, acute phase protein; SAhRM, selective aryl hydrocarbon receptor modulator; DRE, dioxin-response element; DiMNF, 3',4'-dimethoxy- $\alpha$ -naphthoflavone;  $\alpha$ NF,  $\alpha$ -naphthoflavone;  $\beta$ NF,  $\beta$ -naphthoflavone; SAA, serum amyloid associated; PAL, photo-affinity ligand; TCDD, 2,3,7,8-tetrachlorodibenzo-*p*-dioxin; CDTA, 1,2-diaminocyclohexane-*N,N,N',N'*-tetraacetic acid; EAE, experimental acute encephalitis; SGA360, 1-allyl-7-trifluoromethyl-1*H*-indazol-3-yl-4-methoxyphenol; WAY-169916, 4-[1-allyl-7-(trifluoromethyl)-1*H*-indazol-3-yl]benzene-1,3-diol; ARNT, aryl hydrocarbon receptor nuclear translocator; siRNA, small interfering RNA; PCR, polymerase chain reaction; DMSO, dimethyl sulfoxide; ELISA, enzyme-linked immunosorbent assay; IL, interleukin; MOPS, 3-(*N*-morpholino)propanesulfonic acid; Tricine, *N*-[2-hydroxy-1,1-bis(hydroxymethyl)ethyl]glycine.

matory processes. Sustained levels of APP predominantly secreted from the liver can lead to altered immune signaling, cachexia, and amyloidosis. Indeed, in one report, amyloidosis mediated by high levels of SAA expression has been determined to be responsible for the deaths of up to half of patients with juvenile rheumatoid arthritis (Savolainen and Isomäki, 1993). Two APR genes, *SAA1* and *SAA2*, largely mediate the expression of SAA, which is capable of inducing inflammation through binding to Toll-like receptor 2, receptor for advanced glycation end-products, and formyl peptide receptor-like 1 receptors (Cheng et al., 2008). These observations suggest that attenuation of APR in patients with advanced chronic inflammatory diseases may be useful in disease management.

The Aryl hydrocarbon receptor (AHR) is a member of the Per-ARNT-Sim family of transcription factors that are involved in responding to external stimuli (Gu et al., 2000). The AHR is found in the absence of ligand bound to a dimer of 90-kDa heat shock protein and the cochaperone X-associated protein 2 (Petrulis and Perdew, 2002). After binding a ligand, the AHR complex translocates into the nucleus, in which ARNT displaces 90-kDa heat shock protein/X-associated protein 2 and heterodimerizes with AHR. The AHR/ARNT heterodimer is capable of binding to a dioxin-response element (DRE), which can mediate changes in gene transcription. Historically, the AHR target genes that have been most often studied are involved in phase I xenobiotic metabolism. However, an expanding list of AHR target genes involved in a wide range of pathways is emerging (Beischlag et al., 2008). AHR-null mice have revealed that AHR also plays important roles in immune system function, development of liver vasculature, and reproductive success. Furthermore, a survey of the literature indicates that the ligand-activated AHR can enhance and repress specific aspects of inflammatory signaling. For example, the AHR has been shown to control regulatory T cell and  $T_H17$  cell differentiation (Quintana et al., 2008). The use of an AHR antagonist can block  $T_H17$  cell development in vitro, highlighting the possibility that AHR antagonists may have therapeutic potential in chronic inflammatory disease in which  $T_H17$  cells play a key role in disease development (Veldhoen et al., 2009). We have demonstrated that the AHR can attenuate gene expression of a number of acute phase genes in the liver and in hepatic cell lines in the presence of inflammatory signaling (Patel et al., 2009). In addition, this repressive activity occurs in the absence of binding to a DRE, probably through protein-protein interactions.

Nuclear receptors are considered an important therapeutic target for a variety of diseases and in particular have been viewed as targets to inhibit inflammation. The glucocorticoid receptor is commonly activated by corticoid steroids as a means of inhibiting inflammation. The mechanism of this repression is the ability of glucocorticoid receptor ligands to block activator protein-1 and nuclear factor- $\kappa$ B-mediated transcription at the promoters of target genes. However, activation of the glucocorticoid receptor also leads to glucocorticoid response element-driven transcription, which is responsible for the long-term side effects of glucocorticoid receptor agonist exposure. This has led to the development of selective ligands for the glucocorticoid receptor that induce the transrepression response without a response element-mediated induction of gene expression (Schäcke et al., 2004).

This concept has led to the development of a selective estrogen receptor ligand, 4-[1-allyl-7-(trifluoromethyl)-1*H*-indazol-3-yl]benzene-1,3-diol (WAY-169916), which exhibits potent anti-inflammatory activity and has been demonstrated to effectively treat adjuvant induced arthritis (Steffan et al., 2004). We have established that WAY-169916 is also a selective AHR modulator (SAhRM) that is capable of repressing acute-phase gene expression (e.g., *SAA1*, *CRP*, *HP*) without inducing significant DRE-mediated transcriptional activity (Murray et al., 2010b). These results have led to a search for other chemicals that exhibit selective AHR activity. Here, evidence is presented that identifies 3',4'-dimethoxy- $\alpha$ -naphthoflavone (DiMNF) as a SAhRM and demonstrates through structure-activity studies that substitutions on the phenyl ring are determinants for the exhibition of selective AHR activity. DiMNF is capable of repressing APR gene expression without DRE-mediated transcription.

## Materials and Methods

**Materials.** The flavonoid compounds 3',4'-dimethoxy- $\alpha$ -naphthoflavone (2-(2,3-dimethoxyphenyl)-2,3-dihydro-4*H*-benzo[*h*]chromen-4-one) (DiMNF), 4'-hydroxy- $\alpha$ -naphthoflavone (2-(4-hydroxyphenyl)-2,3-dihydro-4*H*-benzo[*h*]chromen-4-one), 2'-methoxy- $\alpha$ -naphthoflavone (2-(2-methoxyphenyl)-2,3-dihydro-4*H*-benzo[*h*]chromen-4-one), 4'-methoxy- $\alpha$ -naphthoflavone (2-(4-methoxyphenyl)-2,3-dihydro-4*H*-benzo[*h*]chromen-4-one),  $\alpha$ -naphthoflavone (2-phenyl-2,3-dihydro-4*H*-benzo[*h*]chromen-4-one), and  $\beta$ -naphthoflavone (3-phenyl-2,3-dihydro-1*H*-benzo[*f*]chromen-1-one) were obtained commercially (Indofine Chemical Co., Hillsborough, NJ). 3'-Methoxy- $\alpha$ -naphthoflavone (2-(3-methoxyphenyl)-2,3-dihydro-4*H*-benzo[*h*]chromen-4-one) was synthesized in-house as described in the chemical synthesis section (Supplemental Fig. S1). The AHR photoaffinity ligand 2-azido-3-[ $^{125}$ I]iodo-7,8-dibromodibenzo-*p*-dioxin (PAL) was synthesized as described previously (Poland et al., 1986). Human recombinant interleukin-1 $\beta$  was obtained commercially (PeproTech, Rocky Hill, NJ). The chemical structures of compounds used in this study are provided in Supplemental Fig. S5.

**Cell Culture.** Huh7, HepG2, and Hep3B human hepatoma cell lines were routinely maintained in  $\alpha$ -modified essential media (Sigma-Aldrich, St. Louis, MO) supplemented with 8% fetal bovine serum (Hyclone Laboratories, Logan, UT) and 100 IU/ml penicillin/100  $\mu$ g/ml streptomycin (Sigma-Aldrich). HepG2 (40/6) human hepatoma stable cell line (Long et al., 1998) containing the stably integrated pGudLuc 6.1 luciferase reporter construct under the control of the murine *Cyp1a1* enhancer were cultured under the same conditions as Huh7 cells. Cells were cultured at 37°C in a humidified atmosphere comprising 95% air and 5% CO<sub>2</sub>.

**Chemical Characterization.** Melting point was recorded on a Fisher-Johns melting point apparatus (Thermo Fisher Scientific, Waltham, MA) and is uncorrected.  $^1$ H NMR spectrum was recorded using a Bruker Avance 500 MHz spectrometer (Bruker, Newark, DE). Chemical shifts ( $\delta$ ) are reported in parts per million downfield from the internal standard. The signals are quoted as d (doublet), t (triplet), m (multiplet) and br s (broad singlet). Mass spectrometry (electron ionization) was determined at the Macromolecular Core facility of Penn State College of Medicine (Hershey, PA). Thin-layer chromatography was developed on aluminum-supported precoated silica gel plates (EM Industries, Gibbstown, NJ).

**3'-Methoxy- $\alpha$ -naphthoflavone Synthesis.** To a solution of 3'-hydroxy- $\alpha$ -naphthoflavone (1.44 g, 5.0 mmol) in acetone (50 ml) were added potassium carbonate (1.38 g, 10 mmol) and dimethyl sulfate (0.95 g, 7.5 mmol) and the reaction was refluxed for 2 h. The reaction mixture was filtered, the filtrate was concentrated, and methylene chloride (100 ml) was added. It was then washed with sodium bicarbonate and water, and the organic layer was dried over MgSO<sub>4</sub> and concentrated under reduced pressure. The crude solid thus obtained

was triturated with diethyl ether and filtered to yield 3'-methoxy- $\alpha$ -naphthoflavone (1.4 g, 93%) as a white solid; melting point, 181 to 182°C;  $^1\text{H}$  NMR (500 MHz,  $\text{CDCl}_3$ ),  $\delta$  3.98 (m, 3H), 7.19 (dd,  $J$  = 8.0 and 2.5 Hz, 1H), 7.45 (br s, 1H), 7.55 (t,  $J$  = 8.5 Hz, 1H), 7.63 (d,  $J$  = 1.5 Hz, 1H), 7.71 (d,  $J$  = 8.0 Hz, 1H), 7.78 to 7.83 (m, 2H), 7.98 (d,  $J$  = 8.5 Hz), 8.03 (dd,  $J$  = 7.0 and 2.5 Hz), 8.22 (d,  $J$  = 8.5 Hz, 1H), 8.69 (d,  $J$  = 8.5 Hz, 1H); mass spectrometry,  $m/z$  (electrospray ionization) 303 ( $\text{M}^+ + 1$ ).

**Luciferase-Based Reporter Assays.** HepG2 (40/6) reporter cells were seeded in six-well plates and cultured to ~80% confluence. Cells were treated as indicated for 4 h and then lysed in 200  $\mu\text{l}$  of lysis buffer [25 mM Tris-phosphate, pH 7.8, 2 mM dithiothreitol, 2 mM CDTA, 10% (v/v) glycerol, and 1% (v/v) Triton X-100]. Lysate (20  $\mu\text{l}$ ) was combined with 80  $\mu\text{l}$  of Luciferase Reporter Substrate (Promega, Madison, WI) and luciferase activity measured with a TD-20e luminometer (Turner Systems, Sunnyvale, CA). Luciferase activity was normalized with respect to protein concentration.

**RNA Isolation and Reverse Transcription.** Total RNA was isolated from cells cultured in six-well plates using TRIzol (Invitrogen, Carlsbad, CA). RNA concentration was determined via spectrophotometry at  $\lambda$  260 and 280 nm. Total RNA (2  $\mu\text{g}$ ) was reverse-transcribed to cDNA using High-Capacity cDNA Archive Kit (Applied Biosystems, Foster City, CA).

**Quantitative PCR.** PCR was performed on a MyiQ (Bio-Rad Laboratories, Hercules, CA) system using PerfeCTa SYBR Green reagent (Quanta Biosciences, Gaithersburg, MD). Quantitative real-time PCR primers (Integrated DNA Technologies, Coralville, IA) used in this study were as follows: *L13A*: forward, CCTGGAGGCGAAGCGGAAA-GAGA, reverse, GAGGACCTCTGTGTATTTGTCAA; *CYP1A1*: forward, TCTTCCTTCGTCCCTTCAC, reverse, TGGTTGATCTGC-CACTGGTT; *SAA1*: forward, AGGCTCAGACAAATACTTCCATGC, reverse, TCTCTGGCATCGCTGATCACTTCT; *C3*: forward, CTCAAT-GTTGACCATGACCG, reverse, AAGTGGTGGAGAAGGTGGTG; *C4*: forward, GGACCCCTGTCCAGTGTTAG, reverse, GTTTGCCTTT-GAGATGGAGG; *C1S*: forward, AAGAGCGTTTTACGGGGTTT, reverse, GTCAGCTGCTTCCACATCAA; *C1R*: forward, ATAGAGGGGACCCAG-GTGCT, reverse, TGGTGGTGTAAACGGAAGTCA; *CYP1B1*: forward, TGCCTGTCACTATTCTCATGCCA, reverse, ATCAAAGTTCTC-CGGGTTAGGCCA; *CYP1A2*: forward, CGGCACTTCGACCTTACAA, reverse, CACATGGCACCAATGACG; *AHRR*: forward, GTGCAATCG-GAACTGCATGGAAA, reverse, TCAGTCTGTTCCTGAGCACAAA; and *UGT1A1*: forward, AACAGGAGCTCATGGCCTCC, reverse, GTTCGCAAGATTTCGATGGTTCG. In all cases, melting point analysis revealed amplification of a single product. Data acquisition and analysis were achieved using MyiQ software (Bio-Rad Laboratories). Quantification was achieved through comparison against target-specific standard curves, and data represent mean fluorescence normalized to that of the control gene ribosomal protein *L13A* to yield a relative mRNA level.

**siRNA-Mediated Knockdown.** siRNA-mediated knockdown of AHR expression in Hep3B cells was performed using the Amara nucleofection system (Lonza Walkersville Inc., Walkersville, MD) with the AHR-specific oligonucleotide sequence (GCACGAGAGGCU-CAGGUUA) ON-TARGETplus siRNA (Dharmacon RNA Technologies, Lafayette, CO) or control green fluorescent protein-specific siRNA oligonucleotide. In brief, cells were washed, and  $2 \times 10^6$  cells were suspended in 100  $\mu\text{l}$  of nucleofection solution, followed by electroporation using program T16. Transfected cells were suspended in 12 ml of complete media and seeded into six-well plates at 2 ml/well. Cells were cultured for 48 h before the addition of indicated treatments. Verification of AHR knockdown was achieved through protein immunoblotting.

**Photoaffinity Competitive Ligand Binding Assay.** Hepatic cytosol extracts were isolated from B6.Cg-Ahr<sup>tm3.1 Bra</sup> Tg (Alb-cre, Ttr-AHR)1GHP "Humanized" AHR mice (Flaveny et al., 2009) by homogenization in 25 mM MOPS, 2 mM EDTA, 0.02%  $\text{NaN}_3$ , and 10% glycerol, pH 7.4, containing 20 mM sodium molybdate and

protease inhibitor cocktail (Sigma-Aldrich) followed by centrifugation at 100,000g for 1 h. All binding experiments were conducted in the dark until photocross-linking of the PAL. In brief, a saturating amount of PAL (0.21 pmol, i.e.,  $8 \times 10^5$  cpm/tube) was added to 150  $\mu\text{g}$  of cytosolic protein. Samples were then incubated with test compounds as indicated for 20 min at room temperature. Samples were photolyzed (402 nm, 8 cm, 4 min), and 1% dextran-coated charcoal was added followed by centrifugation at 3000g for 10 min to remove unbound PAL. Labeled samples were resolved on 8% Tricine polyacrylamide gels, transferred to polyvinylidene difluoride membrane, and visualized by autoradiography. Radioactive AHR bands were excised and quantified by  $\gamma$ -counting.

**Electromobility Shift Assay.** Gel-shift analyses were performed essentially as described previously (Flaveny et al., 2009). In brief, pCI-AHR and pCI-ARNT were in vitro-translated with the TNT-coupled rabbit reticulocyte lysate system (Promega) supplemented with 1.5 mM sodium molybdate. AHR and ARNT (4  $\mu\text{l}$ ) were combined in the presence of 1.5  $\mu\text{l}$  of buffer containing 25 mM HEPES, 1 mM EDTA, 10 mM sodium molybdate, and 10% glycerol, pH 7.5, together with indicated treatments for 30 min at room temperature.  $^{32}\text{P}$ -Labeled DRE probe was added to each reaction and incubated for a further 15 min. Lysates were resolved on 6% DNA-retardation gel (Invitrogen) and visualized by autoradiography.

**Cytotoxicity Assays.** Short-term cytotoxicity was assessed using the 3-(4,5-dimethylthiazol-2-yl)-5-(3-carboxymethoxyphenyl)-2-(4-sulfophenyl)-2H-tetrazolium assay and is based on the mitochondrial reduction of a substrate by viable cells. Huh7 cells were seeded at  $2 \times 10^3$  cell/well, and after overnight incubation, the cells were treated as indicated for a further 48 h. Viability was assessed by adding 40  $\mu\text{l}$ /well 3-(4,5-dimethylthiazol-2-yl)-5-(3-carboxymethoxyphenyl)-2-(4-sulfophenyl)-2H-tetrazolium reagent and determining the absorbance at 490 nm after 2 h. Data represent viable cell number as a percentage of vehicle (DMSO)-treated cells  $\pm$  S.E.M. Longer-term cytotoxicity was determined using a colony-formation assay. For this assay Huh7 cells were seeded at  $1 \times 10^3$  cells/plate, and after overnight incubation, cells were treated as indicated. After 24 h, cells were washed and cultured for an additional 14 days, after which time cells were stained with Coomassie Brilliant Blue for 2 min, and colonies were counted. Data represent the percentage colony number  $\pm$  S.E.M. compared with vehicle (DMSO)-treated controls.

**Anti-human C3 ELISA.** Huh7 cells were seeded in six-well plates and cultured under standard conditions to 70% confluence; at this point cells were transferred to serum-free media supplemented with 5 mg/ml bovine serum albumin. After overnight incubation, cells were treated as indicated for 24 h. Huh7-conditioned media was collected, and aliquots diluted 100-fold in ELISA sample dilution buffer. Diluted samples were analyzed using an anti-human C3 ELISA kit (GenWay Biotech, San Diego, CA) following the manufacturer's instructions. C3 levels were quantified against standard curves ( $R^2$  = 0.99) and concentrations were corrected for the dilution factor and are expressed as mean nanograms per milliliter ( $n$  = 3 per treatment).

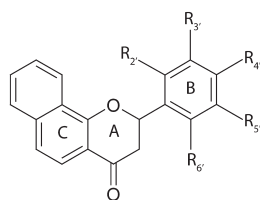
**Molecular Docking Prediction and Binding Energy Calculations.** Binding of  $\alpha$ -NF and DiMNF within the ligand pocket of human and mouse AHR was performed as described previously (Bisson et al., 2009).

**Data Analysis.** In all cases, studies were performed in triplicate. Statistical analyses of data were performed using Prism 5 graphing and statistical analysis software (GraphPad Software Inc., San Diego, CA). Data were analyzed using one-way analysis of variance and Tukey's multiple comparison and Student's  $t$ -tests. All cases in which  $P$  < 0.05 was deemed statistically significant are indicated by an asterisk (\*). Statistical comparisons between different groups are indicated by alphabetical characters.



## Results

**Substitution of the B-Ring of  $\alpha$ NF Affects AHR-Mediated Gene Transcription.** Previous observations using a non-DRE binding mutant of AHR (AHR<sup>A78D</sup>) indicate that ligands for the AHR have the capacity to promote suppression of proinflammatory gene expression in an AHR-dependent, yet DRE-independent, fashion (Patel et al., 2009; Murray et al., 2010b,c). Interestingly, both pure AHR agonists (e.g.,  $\beta$ NF) and the partial agonist/competitive antagonist  $\alpha$ NF elicit the same degree of suppression. These observations prompted us to examine the notion that  $\alpha$ NF may be chemically modified to render it devoid of partial agonist activity, with regard to stimulating DRE-mediated transcription while still retaining its capacity to suppress proinflammatory gene expression in an AHR-dependent manner (i.e., an SAhRM). Previous studies have highlighted the importance of the flavone B-ring in determining AHR agonist potential of flavone-based AHR ligands (Gasiewicz et al., 1996). Therefore, we performed a preliminary quantitative PCR screen of DRE-mediated *CYP1A1* induction in Huh7 cells with  $\alpha$ NF and B-ring derivatives of  $\alpha$ NF: 2'-methoxy- $\alpha$ NF, 4'-methoxy- $\alpha$ NF, 3', 4'-dimethoxy- $\alpha$ NF, and 4'-hydroxy- $\alpha$ NF (Fig. 1). Exposure of Huh7 cells to 10  $\mu$ M  $\beta$ NF or  $\alpha$ NF for 4 h prompted comparable (6- and 5-fold, respectively) increases in the level of *CYP1A1* mRNA compared with vehicle-treated cells alone. Similar treatment of Huh7 cells with B-ring derivatives of  $\alpha$ NF resulted in divergent responses with regard to *CYP1A1* mRNA induction. Substitution for a hydroxyl moiety at the 4'-position ablated *CYP1A1* induction to a level 60% less than that of vehicle-treated cells. Loss of induction was also observed with derivatives substituted with a hydroxyl at the 2' and with the double 3',4'-dimethoxy substitution (Fig. 2). The lack of induction with these derivatives is in contrast to the effect observed with 4'-methoxy- $\alpha$ NF, which induced *CYP1A1* mRNA to a level 60% of the parent compound,  $\alpha$ NF. The inductive capacity of 4'-methoxy- $\alpha$ NF indicates that this derivative is an AHR agonist and thus effectively eliminates this compound as a potential SAhRM.



	R <sub>2</sub> '	R <sub>3</sub> '	R <sub>4</sub> '	R <sub>5</sub> '	R <sub>6</sub> '
$\alpha$ -NF	H	H	H	H	H
2'-methoxy- $\alpha$ -NF	OCH <sub>3</sub>	H	H	H	H
4'-methoxy- $\alpha$ -NF	H	H	OCH <sub>3</sub>	H	H
3', 4'-dimethoxy- $\alpha$ -NF	H	OCH <sub>3</sub>	OCH <sub>3</sub>	H	H
4'-hydroxy- $\alpha$ -NF	H	H	OH	H	H

**Fig. 1.** Chemical structures of  $\alpha$ NF derivatives. Schematic representation of the flavone B-ring derivatives used in this study: DiMNF, 4'-hydroxy- $\alpha$ -naphthoflavone (2-(4-hydroxyphenyl)-2,3-dihydro-4H-benzo[h]chromen-4-one), 2'-methoxy- $\alpha$ -naphthoflavone (2-(2-methoxyphenyl)-2,3-dihydro-4H-benzo[h]chromen-4-one), 4'-methoxy- $\alpha$ -naphthoflavone (2-(4-methoxyphenyl)-2,3-dihydro-4H-benzo[h]chromen-4-one), 3'-methoxy- $\alpha$ -naphthoflavone (2-(3-methoxyphenyl)-2,3-dihydro-4H-benzo[h]chromen-4-one), and  $\alpha$ -naphthoflavone (2-phenyl-2,3-dihydro-4H-benzo[h]chromen-4-one).

The diverse responses observed suggest that minor modifications of the parent compound can exert a profound effect on AHR function and associated *CYP1A1* transcription.

**B-Ring Derivatives of  $\alpha$ NF Antagonize DRE-Mediated Gene Expression.** *CYP1A1* expression is predominantly driven in response to ligand-transformed AHR binding in conjunction with ARNT to its cognate response elements (DRE) located in the *CYP1A1* upstream enhancer region. We therefore examined whether the inhibitory effect of the 2'-methoxy-, 4'-hydroxy-, and 3',4'-dimethoxy- $\alpha$ NF derivatives is a consequence of diminished AHR/ARNT/DRE binding, a defining characteristic of the SAhRMs characterized previously. Consistent with the *CYP1A1* mRNA expression analysis, electromobility shift studies using in vitro translated components revealed a marked decrease in AHR/ARNT heterodimer binding to a DRE oligonucleotide probe, relative to that observed with the positive binding controls  $\alpha$ NF and  $\beta$ NF (Fig. 3). The complementary lack of AHR/ARNT/DRE complex formation and *CYP1A1* mRNA induction may indicate the potential for these derivatives to exert SAhRM activity or may reflect an inability to bind the AHR. To discriminate between these two possibilities, we performed a series of DRE-mediated reporter ligand competition assays. HepG2 (40/6) cells, stably integrated with the DRE containing *Cyp1a1* enhancer upstream of a luciferase reporter, were treated for 4 h with vehicle, 2 nM TCDD, or in conjunction with 1  $\mu$ M substituted  $\alpha$ NF derivatives, and luciferase activity was determined (Fig. 4). Each of the test compounds was able to elicit an antagonistic effect with regard to AHR-dependent, DRE-mediated reporter expression; however, the magnitude of the inhibition varied with the  $\alpha$ NF derivative used. 4'-Hydroxy- $\alpha$ NF inhibited TCDD-induced reporter activity by 93%, whereas 2'-methoxy- $\alpha$ NF exhibited 97% repression. The highest level of antagonism was displayed by DiMNF, achieving 98% repression. The ability of these derivatives to compete with TCDD and antagonize DRE-mediated reporter expression suggests that substitution on the flavone B-ring may alter AHR-binding

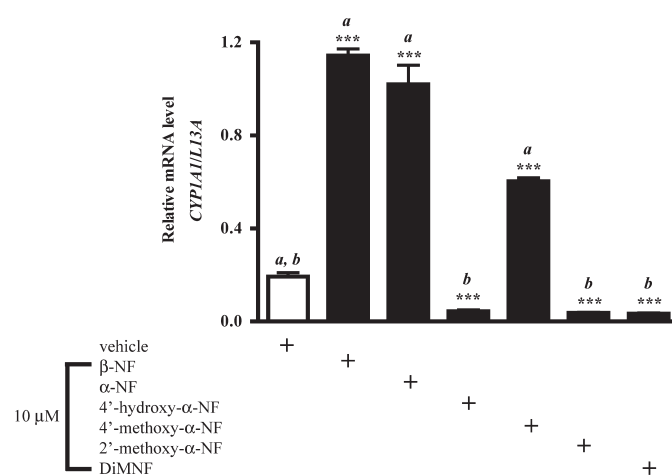


**Fig. 2.** Derivatives of  $\alpha$ NF exhibit differential AHR agonist activity at the *CYP1A1* promoter. Huh7 cells were exposed to vehicle (DMSO), 10  $\mu$ M  $\beta$ NF,  $\alpha$ NF, 4'-hydroxy- $\alpha$ NF, 4'-methoxy- $\alpha$ NF, 2'-methoxy- $\alpha$ NF, or DiMNF for 4 h, and *CYP1A1* mRNA expression was analyzed by quantitative PCR. Data represent mean *CYP1A1* mRNA  $\pm$  S.E.M. normalized to the constitutively expressed ribosomal L13A mRNA. Statistical significance is indicated by an asterisk (\*,  $P < 0.05$ ; \*\*,  $P < 0.01$ ; \*\*\*,  $P < 0.001$ ). Intertreatment statistical comparisons are indicated by lowercase letters.

affinity and indicates that failure of these derivatives to stimulate AHR/ARNT/DRE binding and *CYP1A1* induction is possibly a consequence of competition for the ligand binding pocket of the AHR. With the exception of 4'-methoxy- $\alpha$ NF, all of the derivatives demonstrated no *CYP1A1* induction; however, DiMNF seemed to be the most promising SAHRM candidate because of its greater antagonistic activity and thus was examined in further detail.

**DiMNF Is an AHR Ligand.** The capacity of DiMNF to competitively antagonize TCDD-mediated AHR transactivation is indicative but not conclusive evidence that DiMNF is a direct AHR ligand. To definitively characterize the ligand status of DiMNF, in vitro competitive ligand binding assays were performed against the AHR photoaffinity ligand PAL. Hepatic-derived cytosolic extracts isolated from "humanized" AHR C57/BJ6 mice were incubated with 200 pM [ $^{125}$ I]PAL in combination with increasing concentrations of either the parent compound  $\alpha$ NF or its substituted derivative DiMNF and the magnitude of competition assessed radiometrically (Fig. 5). The data obtained revealed nearly identical ligand competition profiles for  $\alpha$ NF and DiMNF, with  $IC_{50}$  at 25 and 21 nM, respectively (Fig. 5, A and B). Such data corroborate the observed antagonism of TCDD-mediated reporter gene expression by both  $\alpha$ NF and DiMNF. In addition, competition for PAL binding indicates that DiMNF interacts with the ligand binding pocket of AHR and thus represents an AHR ligand. Furthermore, the similar  $IC_{50}$  values for  $\alpha$ NF and DiMNF indicate that the differential effects with regard to agonist/antagonistic DRE-mediated expression are unlikely to be a consequence of relative binding affinities.

The establishment of DiMNF as an AHR ligand with apparent antagonistic activity with regard to DRE-mediated gene expression raised the issue of whether DiMNF is acting directly as an intrinsic antagonist or rather whether it is metabolized to an intermediate, which also has AHR ligand status and is the actual source of antagonism. To address the issue of DiMNF metabolism, DRE-mediated reporter dose-response and competitive time course assays were conducted (Fig. 6, A and B). HepG2 (40/6) cells were incubated for 4 h with vehicle, 2 nM TCDD, or TCDD plus increasing concentrations of DiMNF, and reporter activity was quantified. Exposure to TCDD yielded a 90-fold increase in activity over

vehicle-treated control. Coincubation with TCDD and increasing concentrations of DiMNF prompted a significant dose-dependent decrease in reporter activity (Fig. 6A). HepG2 (40/6) cells were incubated with 2 nM TCDD or TCDD in combination with 10  $\mu$ M DiMNF, and reporter activity was determined over 4, 8, and 16 h. Increasing exposure to TCDD resulted in a time-dependent decrease in reporter activity, consistent with the well characterized TCDD-mediated turnover of AHR protein. Extended incubation with TCDD and DiMNF again demonstrated the competitive antagonist response with regard to TCDD-mediated reporter induction (Fig. 6B). However, a time-dependent increase in reporter activity was observed, suggesting a loss of DiMNF competition, perhaps signifying metabolic conversion of DiMNF into a noncompetitive intermediate. These observations argue against the notion that DiMNF may undergo spontaneous or metabolic conversion to generate a product responsible for AHR antagonism.

**The AHR Gene Battery Is Minimally Influenced by DiMNF.** Among the cohort of gene targets that comprise the DRE-mediated AHR battery, induction of *CYP1A1* is considered the predominant biomarker of AHR activation. However, there are limited data indicating differential induction of the AHR battery depending on the AHR ligand used. We therefore examined whether the failure of DiMNF to stimulate DRE-mediated expression is restricted to *CYP1A1* or universal with regard to the DRE-mediated AHR battery. Huh7 cells were exposed to vehicle or 10  $\mu$ M DiMNF for 3 h, and the expression of *CYP1A1*, *CYP1B1*, *CYP1A2*, *AHR*, and *UGT1A1* mRNA was examined by quantitative PCR (Fig. 7). For each gene examined, treatment with DiMNF failed to significantly induce mRNA expression above the vehicle-treated control baseline. Indeed, DiMNF prompted a decrease in basal expression levels, which was particularly evident with *CYP1A1* and *UGT1A1*; although decreases in basal expression were observed with the other AHR target genes examined, these proved to be statistically insignificant. Cytotoxicity assays revealed a slight inhibitory effect of DiMNF upon cell survival, which fails to account for the absence of DRE-mediated induction in response to DiMNF (Supplemental Fig. S2). The mechanism by which DiMNF exerts this modest cytotoxic effect remains to be explored.

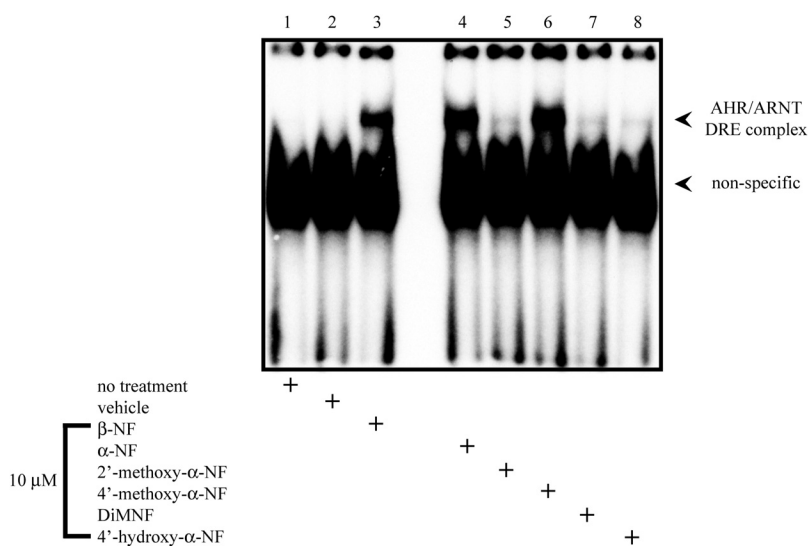


**Fig. 3.** The agonist activity of B-ring derivatives of  $\alpha$ NF correlates with AHR binding to its cognate response element. Ligand-mediated DRE binding by the AHR/ARNT heterodimer was assessed by electromobility shift assay using in vitro-translated components. Equal volumes of translated human AHR and ARNT were combined and incubated for 30 min at room temperature with vehicle (DMSO) (lane 2), 10  $\mu$ M  $\beta$ NF and  $\alpha$ NF as positive controls (lanes 3 and 4), or 10  $\mu$ M 2'-methoxy- $\alpha$ NF (lane 5), 4'-methoxy- $\alpha$ NF (lane 6), DiMNF (lane 7), and 4'-hydroxy- $\alpha$ NF (lane 8). Samples were then incubated for 15 min with [ $^{32}$ P]DRE probe encompassing the murine *Cyp1a1* DRE enhancer before resolving on 8% nondenaturing DNA retardation gels. Gels were fixed and dried under vacuum and exposed to autoradiographic film. AHR/ARNT/DRE and nonspecific complexes are as indicated.

These data indicate that the lack of induction elicited by DiMNF is not restricted to *CYP1A1* and probably will apply to the majority of DRE-mediated gene targets.

**DiMNF Effectively Suppresses Cytokine-Mediated Inflammatory Gene Expression.** Transcriptional regulation by AHR is not limited to mechanisms involving its cog-

nate response element. Previous data have demonstrated that IL1 $\beta$ -mediated induction of the acute phase protein *SAA1* can be significantly diminished in an AHR-dependent, DRE-independent manner. Moreover, such suppression can be evoked selectively (i.e., in the absence of DRE-mediated gene expression) with the SAhRM class of AHR ligands. We therefore examined the potential of DiMNF to inhibit *SAA1* expression in response to a proinflammatory challenge (Fig. 8A). Huh7 cells exposed to 2 ng/ml IL1 $\beta$  for 3 h prompted a significant increase in *SAA1* mRNA expression compared with vehicle alone, as determined through quantitative PCR analysis. Pre-incubation with 10  $\mu$ M DiMNF for 1 h before challenging with IL1 $\beta$  resulted in a significant suppression of *SAA1* mRNA expression. The establishment of DiMNF as an effective suppressor of cytokine-mediated *SAA1* expression led us to examine the structure-activity relationship associated with the 3' and 4' methoxy moieties with regard to *SAA1* expression. The 3'-methoxy derivative was synthesized as described under *Materials and Methods* and was tested against its 4'-methoxy and 3',4'-dimethoxy counterparts. Huh7 cells exposed to 2 ng/ml IL1 $\beta$  for 3 h prompted a 20-fold increase in *SAA1* mRNA (Fig. 8B). Treatment with each of the three methoxy derivatives for 1 h before IL1 $\beta$  resulted in a marked and significant suppression of *SAA1* mRNA associated with each derivative (Fig. 8B).

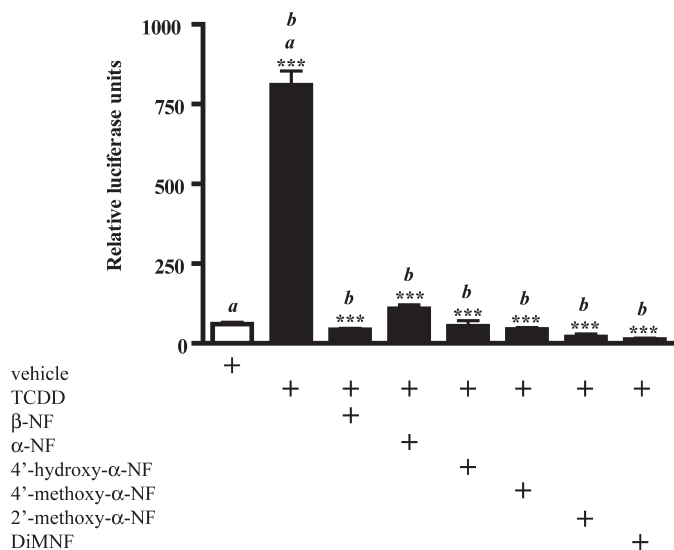


**Fig. 4.** Derivatives of  $\alpha$ NF are antagonistic toward TCDD-mediated gene expression in the context of a heterologous DRE reporter construct. HepG2 (40/6) cells were exposed to vehicle (DMSO), 10  $\mu$ M  $\beta$ NF,  $\alpha$ NF, 4'-hydroxy- $\alpha$ NF, 4'-methoxy- $\alpha$ NF, 2'-methoxy- $\alpha$ NF, or DiMNF just before addition of 10 nM TCDD. Cells were incubated for 5 h, and luciferase activity was assayed. Data represent mean relative luciferase units  $\pm$  S.E.M. Statistical significance is indicated by an asterisk (\*,  $P < 0.05$ , \*\*,  $P < 0.01$ , and \*\*\*,  $P < 0.001$ ). Intertreatment statistical comparisons are indicated by lowercase letters.

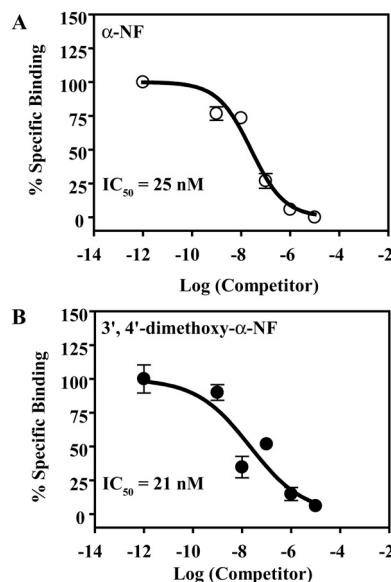


**Fig. 5.** DiMNF is a competitive ligand for the human AHR with binding characteristics similar to those of  $\alpha$ NF. Competitive ligand binding assays were performed using hepatic cytosol from "humanized AHR" C57B/6J mice. Cytosolic extracts were incubated with increasing concentrations of either  $\alpha$ NF (A) or DiMNF (B) in the presence of the AHR photoaffinity ligand. After exposure to UV radiation to facilitate covalent cross-linking, samples were resolved by Tricine SDS-polyacrylamide gel electrophoresis and transferred to membrane. After exposure to film, AHR bands were excised and quantified through  $\gamma$ -counting. Data represent direct mean counts per million  $\pm$  S.E.M.

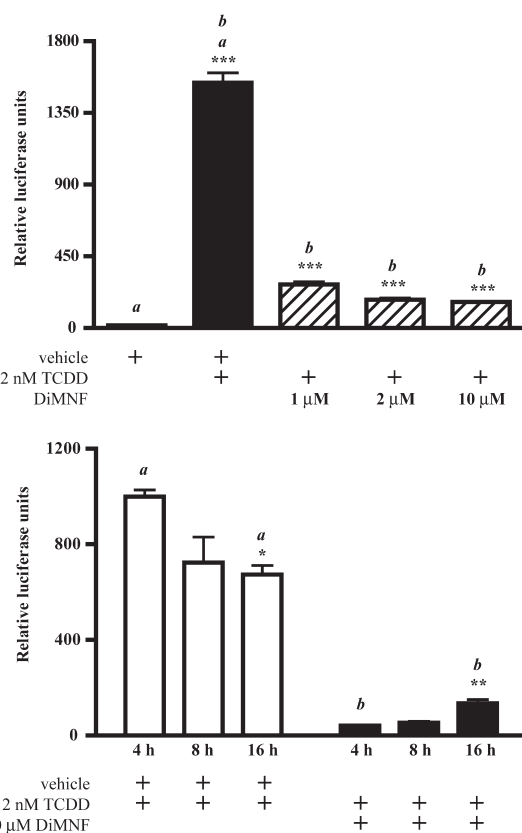


**Fig. 6.** Competitive antagonism of ligand-mediated DRE activity by DiMNF is dose- and time-dependent. A, HepG2 (40/6) cells were exposed to vehicle (DMSO) or 1, 2, or 10  $\mu$ M DiMNF just before the addition of 2 nM TCDD. Cells were incubated for 5 h, and luciferase activity was assayed. B, HepG2 (40/6) cells were exposed to vehicle (DMSO) or 10  $\mu$ M DiMNF just before the addition of 2 nM TCDD. Cells were incubated, and luciferase activity was assayed after 4, 8, and 16 h. Data represent mean relative luciferase units  $\pm$  S.E.M. Statistical significance is indicated by an asterisk (\*,  $P < 0.05$ , \*\*,  $P < 0.01$ , and \*\*\*,  $P < 0.001$ ). Intertreatment statistical comparisons are indicated by lowercase letters.

Previous microarray studies using the A78D non-DRE binding AHR mutant identified additional inflammatory gene targets suppressed in response to ligand activation, including members of the complement cascade [i.e., *complement factor 3 (C3)* or *acylation-stimulating protein cleavage product*, *complement factor 4 (C4)*, *complement component C1, s subcomponent (C1S)*, and *complement component C1, r*

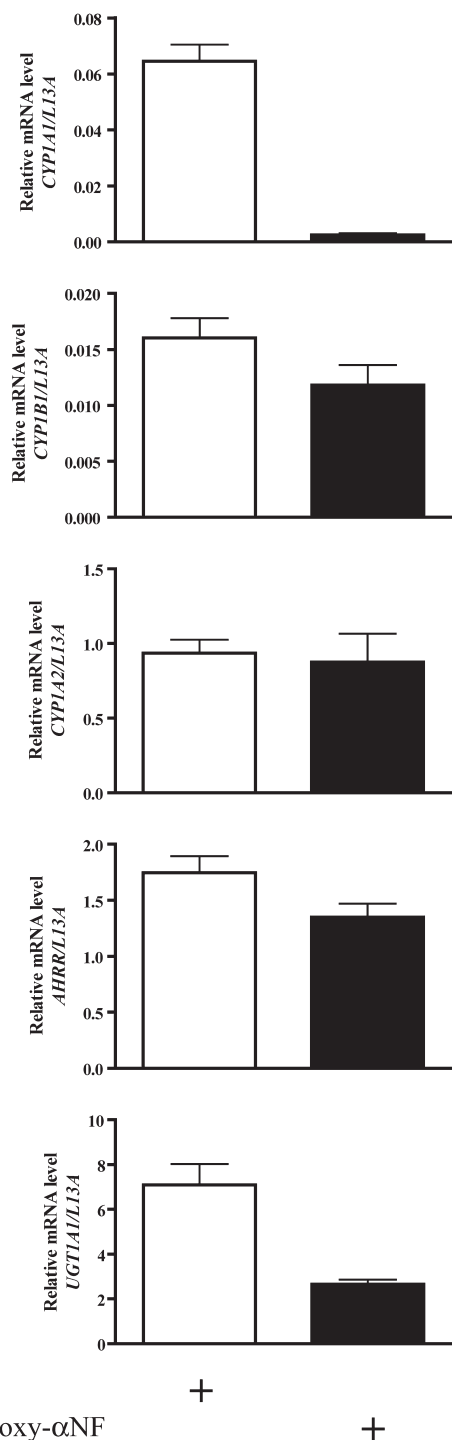


**Fig. 7.** Lack of DRE-dependent agonist activity by DiMNF is conserved across the AHR gene battery. Huh7 cells were incubated with vehicle (DMSO) or 10  $\mu$ M DiMNF for 4 h and CYP1A1, CYP1B1, CYP1A2, AHR, and UGT1A1 mRNA expression was analyzed by quantitative PCR. Data represent mean target mRNA  $\pm$  S.E.M. normalized to the constitutively expressed ribosomal L13A mRNA.

*subcomponent (C1R)*] (Patel et al., 2009). We therefore investigated the capacity of DiMNF to influence inflammatory targets other than SAA1. Huh7 cells exposed to 2 ng/ml IL1 $\beta$  for 3 h stimulated the transcription of C4, C1S, C1R, and C3 above vehicle-treated controls by 6-, 7-, 2-, and 10-fold, respectively (Fig. 9A). The magnitude of IL1 $\beta$ -mediated mRNA induction of each of the complement factors was significantly reduced in response to 1-h preincubation with 10  $\mu$ M DiMNF; in all cases, mRNA expression was diminished by more than 50%. Suppression of IL1 $\beta$ -mediated C3 mRNA expression by DiMNF was also examined at the protein level. Huh7 cells were incubated with vehicle, 2 ng/ml IL1 $\beta$ , or IL1 $\beta$  in combination with 10  $\mu$ M DiMNF. After 24 h, cell culture media samples were analyzed for secreted C3 protein content by ELISA (Fig. 9B). The basal level of C3 protein in vehicle-conditioned media was determined to be 123 ng/ml, which increased 328% to 403 ng/ml in IL1 $\beta$ -conditioned media. Exposure to DiMNF before IL1 $\beta$  significantly decreased the level of secreted C3 protein in conditioned media by 40% to 247 ng/ml relative to IL1 $\beta$  alone. Thus, these data validate

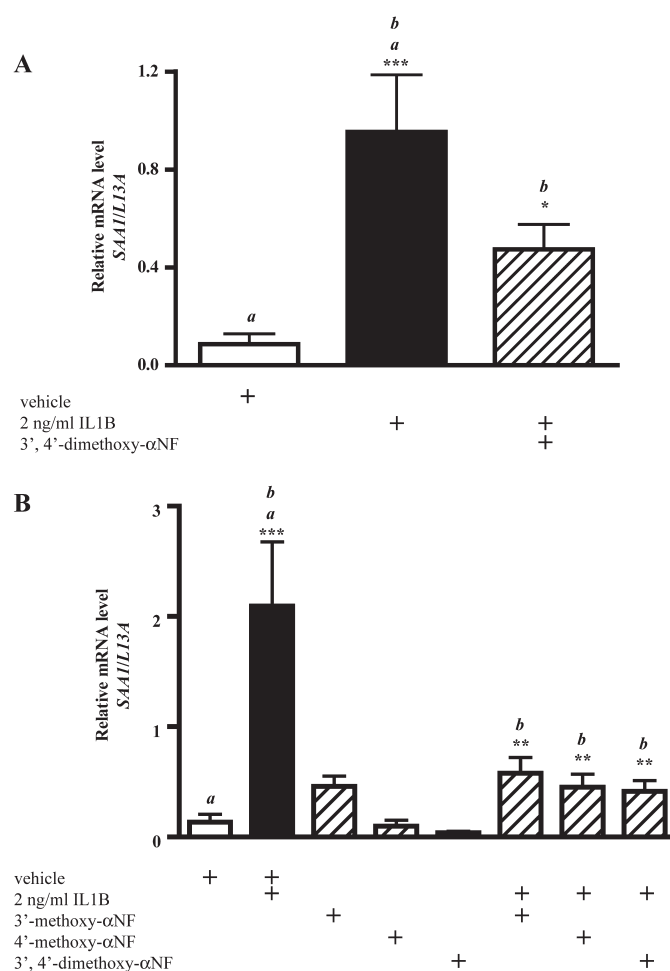


**Fig. 8.** DiMNF exhibits repressive activity toward cytokine-mediated SAA1 induction. Huh7 cells were incubated with vehicle (DMSO) or 10  $\mu$ M DiMNF (A) or 10  $\mu$ M 3'-methoxy- $\alpha$ NF, 4'-methoxy- $\alpha$ NF, or DiMNF (B) for 1 h before stimulation with 2 ng/ml human IL1 $\beta$ . Cells were incubated for an additional 4 h, and SAA1 mRNA expression was analyzed by quantitative PCR. Data represent mean SAA1 mRNA  $\pm$  S.E.M. normalized to the constitutively expressed ribosomal L13A mRNA. Statistical significance is indicated by an asterisk (\*,  $P < 0.05$ , \*\*,  $P < 0.01$ , and \*\*\*,  $P < 0.001$ ). Intertreatment statistical comparisons are indicated by lowercase letters.



the microarray observation that ligand-activation of AHR results in the attenuation of cytokine-mediated *SAA1* and complement component mRNA expression. Furthermore, in

the context of *C3*, these data also demonstrate that transcriptional repression of mRNA is reflected at the level of protein secretion and thus may have biological implications. Despite

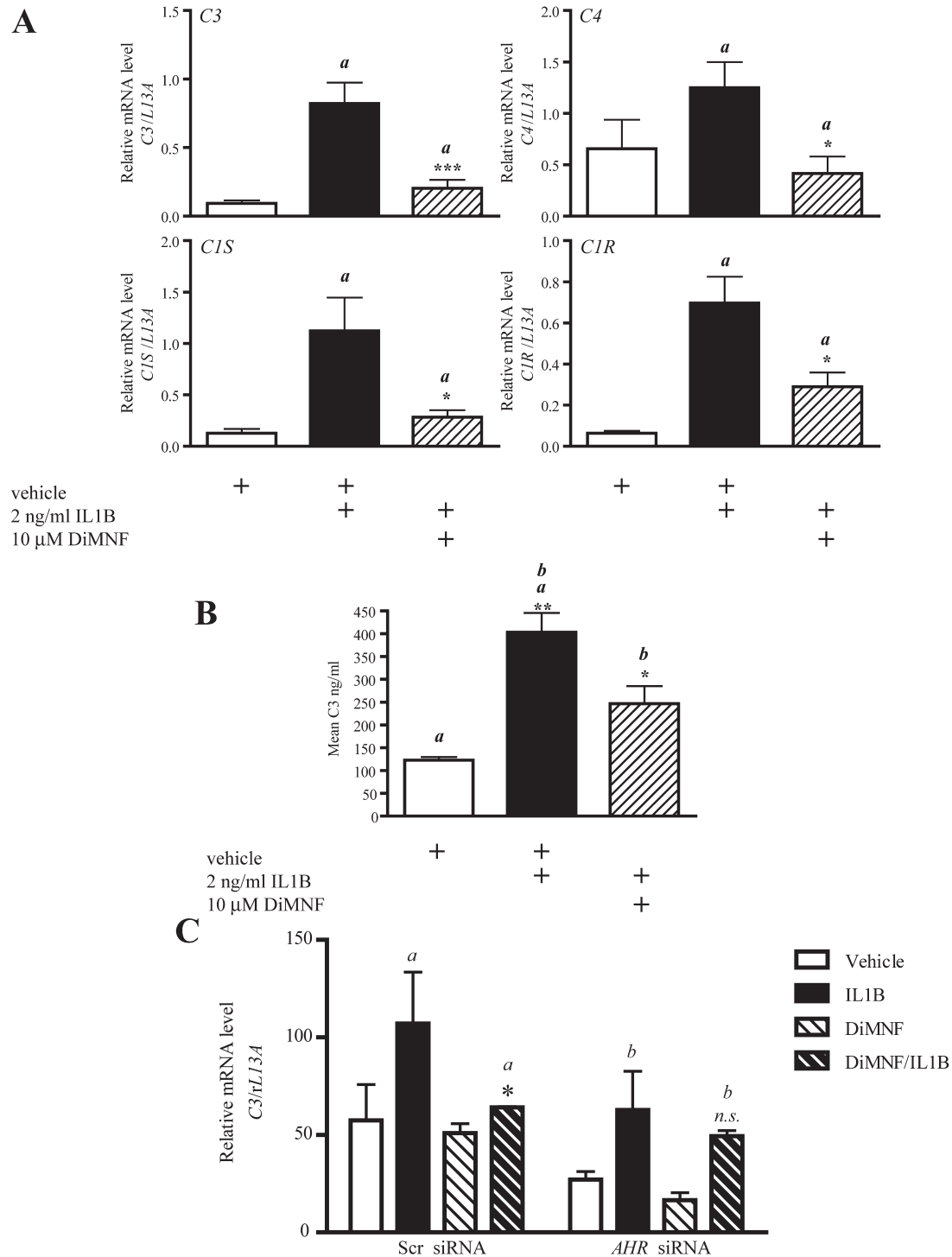


**Fig. 9.** Complement gene expression is a target for AHR-dependent DiMNF-mediated suppression. **A**, Huh7 cells were incubated with vehicle (DMSO) or 10  $\mu$ M DiMNF for 1 h before stimulation with 2 ng/ml human IL1 $\beta$ . Cells were incubated for an additional 4 h, and C3, C4, C1S, and C1R mRNA expression was analyzed by quantitative PCR. Data represent mean C3, C4, C1S, and C1R mRNA  $\pm$  S.E.M. normalized to the constitutively expressed ribosomal L13A mRNA. **B**, Huh7 cells were incubated with vehicle (DMSO) or 10  $\mu$ M DiMNF for 1 h before stimulation with 2 ng/ml human IL1 $\beta$ . After 24-h incubation, conditioned media were analyzed for C3 protein content by ELISA, and C3 concentrations were extrapolated from the standard curve. Data represent mean media C3 concentration (nanograms per milliliter)  $\pm$  S.E.M. **C**, Hep3B cells targeted with scrambled or AHR-specific siRNA were incubated with vehicle (DMSO) or 10  $\mu$ M DiMNF for 1 h before stimulation with 2 ng/ml human IL1 $\beta$ . Cells were incubated for an additional 4 h, and C3 mRNA expression was analyzed by quantitative PCR. Data represent mean C3 mRNA  $\pm$  S.E.M. normalized to the constitutively expressed ribosomal L13A mRNA. Statistical significance is indicated by an asterisk (\*,  $P < 0.05$ , \*\*,  $P < 0.01$ , and \*\*\*,  $P < 0.001$ ). Intertreatment statistical comparisons are indicated by lowercase letters.



demonstrating through competitive ligand binding assays that DiMNF represents a bona fide AHR ligand, we wished to examine AHR-dependence with regard to DiMNF-mediated C3 mRNA suppression. To achieve this aim, siRNA-mediated knockdown of AHR expression was performed in Hep3B cells before exposure to DiMNF. Confirmation of AHR ablation was demonstrated through AHR immunoblot analysis, which revealed an 80% decrease in AHR protein expression relative to scrambled siRNA controls (Supplementary Fig. S3A). To validate that a functional level of knockdown was achieved, TCDD-mediated *CYP1A1* induction was determined in AHR-targeted siRNA-treated cells. Ablation of AHR protein expression significantly diminished both basal and TCDD-mediated *CYP1A1* mRNA induction, thus indicating a functional suppression of AHR activity (Supplementary Fig. S3B). Exposure of scrambled siRNA and AHR-depleted Hep3B cells with 2 ng/ml IL1 $\beta$  for 4 h prompted an induction of C3 mRNA. Although basal and induced C3 mRNA levels in AHR-depleted cells were lower than in their scrambled siRNA counterparts, the relative induction after IL1 $\beta$  treatment remained similar (Fig. 9C). Preincubation of scrambled siRNA Hep3B cells for 1 h with 10  $\mu$ M DiMNF before 4-h IL1 $\beta$  exposure resulted in a marked and significant suppression of C3 mRNA expression. However, the same DiMNF/IL1 $\beta$  treatment in AHR-depleted Hep3B cells failed to result in significant suppression of C3 mRNA expression (Fig. 9C). Such data indicate that DiMNF-mediated suppression of cytokine-dependent C3 induction requires the functional expression of AHR.

**DiMNF Adopts a Unique Orientation within the Ligand Binding Pocket of AHR.** Despite nearly identical AHR binding affinity, the divergent SAhRM activity exhibited by DiMNF, compared with its partial agonist/competitive antagonist parent compound  $\alpha$ NF, attests to a fundamental difference that influences and directs AHR functionality. Using an in silico modeling approach based on a lowest energy ligand docking algorithm validated previously with other AHR ligands (Bisson et al., 2009), we examined the spatial and energy profiles of  $\alpha$ NF and DiMNF within the ligand binding pocket of human and mouse AHR (Fig. 10 and Supplemental Fig. S4). Under the parameters of the model,  $\alpha$ NF docked into the binding pocket with a binding energy of  $-4.26$  kcal/mol (mouse AHR) and  $-4.06$  kcal/mol (human AHR), establishing a hydrogen bond between the A-ring carbonyl oxygen (C=O) and the hydroxyl hydrogen (OH) of residue Ser359 (mouse)/Ser365 (human). DiMNF docked into the binding pocket with a higher binding energy than  $\alpha$ NF in both species of AHR,  $-6.1$  kcal/mol (mouse) and  $-5.44$  kcal/mol (human). The stronger binding energy exhibited by DiMNF seems to be a consequence of the introduction of an additional hydrogen bond spanning the oxygen of the 3'-methoxy (OCH<sub>3</sub>) moiety and the hydroxyl hydrogen (OH) of residue Thr283 (mouse)/Thr289 (human). These docking analyses predict a stronger, more energetically favorable interaction between DiMNF and the ligand binding pocket of AHR compared with that observed with its parent compound  $\alpha$ NF. We also examined the docking parameters associated with 4'-methoxy- $\alpha$ NF, which, unlike its dimethoxy counterpart DiMNF, exhibited a marked degree of agonist activity in the initial quantitative PCR *CYP1A1* and electromobility shift assay screens (Figs. 2. and 3). The docking model predicted a binding orientation similar to that observed with

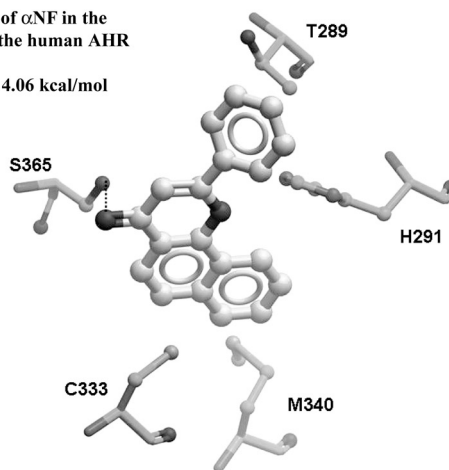
DiMNF but with a reduced binding energy of  $-5.15$  kcal/mol (mouse)/ $-5.14$  kcal/mol (human). The energy reduction observed with 4'-methoxy- $\alpha$ NF may be due to the absence of the 3'-methoxy/Thr283/289 hydrogen bond found with DiMNF.

## Discussion

Both naturally occurring and synthetic polyphenolic flavonoid classes of compounds are recognized as abundant sources of ligands for the AHR (Ashida et al., 2008). Flavonoid AHR ligands exhibit divergent responses with regard to canonical DRE-mediated AHR activity; some [e.g.,  $\beta$ -naphthoflavone (Gillner et al., 1985) and quercetin (Ciolino et al., 1999)] demonstrate agonist activity; others [e.g.,  $\alpha$ -naphthoflavone (Gillner et al., 1985), 6,2',4'-trimethoxyflavone (Murray et al., 2010a), and kaempferol (Ciolino et al., 1999)] are partial agonists or competitive antagonists (Lu et al., 1995, 1996; Zhang et al., 2003). A large body of evidence describes the anti-inflammatory, tumor-suppressing, and general beneficial activity of flavonoids, typically attributed to their free-radical scavenging antioxidant activity or through blockade of mitogenic kinase signaling (Cho et al., 2003; Van Dross et al., 2005; García-Lafuente et al., 2009). However, despite the

Predicted binding of  $\alpha$ NF in the binding pocket of the human AHR

Binding Energy:  $-4.06$  kcal/mol



Predicted binding of 3',4'-dimethoxy- $\alpha$ NF in the binding pocket of the human AHR

Binding Energy:  $-5.44$  kcal/mol

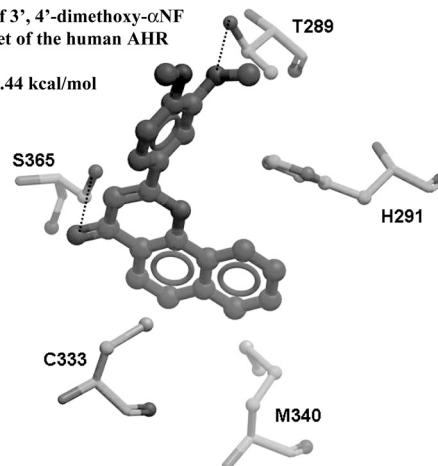


**Fig. 10.** In silico ligand docking algorithm predicts differential orientations between  $\alpha$ NF and the SAhRM DiMNF in the ligand binding pocket of AHR. Predicted docking orientations of  $\alpha$ -NF (A) and DiMNF (B) within the proposed ligand binding pocket of human AHR, highlighting common interaction with 365 but divergent interaction with Thr289 and 3',4'-dimethoxy- $\alpha$ NF.

AHR binding status of many flavonoids, it is unclear whether some of the positive aspects are in any way mediated through the AHR (Zhang et al., 2003). Recent evidence has expanded the repertoire of physiological processes influenced by the AHR to include hematopoietic development, inflammatory cytokine and acute phase reactant expression,  $T_H1/2$  balance, and  $T_H17$  and  $T_{Reg}$  development. Thus, it is intriguing to hypothesize that some of the positive anti-inflammatory effects of flavonoids are mediated through the AHR and its emerging role in modulating immunological processes (Veldhoen et al., 2008; Jux et al., 2009; Kerkvliet et al., 2009; Patel et al., 2009; Sekine et al., 2009; Singh et al., 2009; Boitano et al., 2010).

The recent characterization of an anti-inflammatory SAhRM, which represents a novel subset of AHR ligands with the capacity to dissociate non-DRE dependent anti-inflammatory action of AHR from potentially undesirable DRE-mediated transactivation points to the amelioration of inflammatory conditions through pharmacological modulation of AHR (Murray et al., 2010c). The modulation of AHR and resultant beneficial effects has also been demonstrated with AHR agonists such as TCDD in diminishing inflammatory parameters associated with a genetic model of diabetes (Kerkvliet et al., 2009). However, systemic toxicity is probably with full agonists but will not be as evident with weak agonists such as 6-methoxychlorodibenzofuran, which exhibits antitumor properties in models of breast and prostate cancer (Zhang et al., 2009). It is probable that AHR agonists are exerting some of these effects through non-DRE dependent mechanisms akin to the dissociative SAhRMs. The anti-inflammatory properties of flavonoids and their propensity to bind AHR have led us to examine whether flavonoids can exhibit the dissociated transcriptional characteristics of an SAhRM. The observation that the partial AHR agonist  $\alpha$ NF can suppress cytokine-mediated inflammatory gene expression (e.g., SAA1) suggests that its structure may be modified to diminish agonist activity while retaining its AHR-mediated anti-inflammatory properties, thus generating a flavonoid-based SAhRM. Previous data have indicated that substitution of the flavone B-ring at the 3' and 4' positions contributes significantly to enhanced AHR affinity in conjunction with increased antagonism of DRE-mediated responses (Gasiewicz et al., 1996; Henry et al., 1999). The screens used in this study confirm that targeted substitution can alter AHR responsiveness, thus diminishing the agonist potential of  $\alpha$ NF. The initial screen with hydroxyl- and methoxy-derivatives of  $\alpha$ NF revealed a marked reduction in *CYP1A1* induction relative to the parent compound  $\alpha$ NF and full agonist  $\beta$ NF. Loss of agonist activity together with competitive inhibition of TCDD-mediated induction was also observed in a DRE-mediated reporter gene context. These assays used the *CYP1A1* enhancer, which is restricted to AHR response elements, suggesting that the lack of induction by  $\alpha$ NF derivatives is unlikely to be a consequence of suppression through additional non-AHR response elements, such as antioxidant or estrogen receptor response elements, which are reported to be sensitive to various flavonoids (Kuiper et al., 1998). The diminished induction of AHR target genes (e.g., *CYP1A1* and *AHRR*) elicited by the inhibitory B-ring derivatives in general and DiMNF in particular correlates with a loss of binding of the AHR/ARNT heterodimer to its cognate response element, as evidenced through gel retardation

assays. Inhibition of the AHR/ARNT/DRE complex formation is observed with the previously characterized SAhRMs WAY-169916 and 1-allyl-7-trifluoromethyl-1*H*-indazol-3-yl-4-methoxyphenol (SGA360) and thus may be a defining characteristic of an SAhRM (Murray et al., 2010b,c). The mechanism by which WAY-169916, SGA360, and other putative SAhRMs (e.g., DiMNF) fail to mediate AHR/ARNT/DRE binding has not been elucidated. AHR turnover studies in the presence of WAY-169916, DiMNF, and other weak agonists/antagonists reveal that AHR is more resistant to ligand-mediated receptor degradation compared with TCDD or other potent agonists (I. Murray, unpublished data). Such data argue against AHR turnover to account for diminished DRE interaction and associated gene induction. The absence of DRE binding suggests that DiMNF will restrict the expression of all DRE-regulated gene targets within the AHR battery and that inhibition is not limited to those targets currently examined. Loss of DRE complex formation may arise as a consequence of diminished affinity of SAhRM-bound AHR for ARNT, either through a direct nonpermissive conformational change in ligand-bound AHR or indirectly through inefficient nuclear translocation that could limit interaction with ARNT. We are investigating these possibilities to assess how DiMNF and other putative SAhRMs differentially influence AHR activity relative to typical AHR ligands to ablate DRE-mediated transactivation. Evidence for a specific repressive AHR conformation is contradictory, preliminary ligand modeling data predict the formation of a novel hydrogen bond between DiMNF (and WAY-169916, together with other putative SAhRMs being investigated) and Thr283/289 (mouse/human), which is absent with  $\alpha$ NF and typical AHR ligands. Such an interaction may impart a unique conformational change in AHR and be the basis for non-DRE selectivity. Mutational analysis may verify the importance of this residue in determining selectivity with the caveat that mutation around the ligand binding pocket is often detrimental to binding affinity (Pandini et al., 2009). Typical AHR agonists also have the capacity to suppress those inflammatory gene targets repressed by SAhRMs; thus, non-DRE mediated suppression may be a function of ligand binding itself rather than a specific mode of interaction. Should this be the case, the basis for selectivity is a loss of function (i.e., non-DRE binding phenomenon) rather than a gain of function (i.e., pharmacological acquisition of repressive potential). Such loss of function may explain the reported physiological suppressive effects of AHR with regard to immune signaling, because any putative endogenous AHR ligand should also elicit DRE-independent repression (Jux et al., 2009; Sekine et al., 2009). Thus, the direction of AHR action becomes context-specific, defined not by ligand binding alone but requiring additional as-yet-unidentified components. However, the various B-ring derivatives examined here indicate profound effects on AHR selectivity (e.g., 4'-methoxy- versus 4'-hydroxy- $\alpha$ NF) despite having similar binding affinities to the parent compound, with the conclusion that differences are being transmitted through ligand binding. Refinement of the predictive ligand binding model using additional compounds that exhibit SAhRM characteristics or the realization of a crystal structure for the AHR may yet illuminate subtle conformational differences evoked by different classes of AHR ligand.



The capacity of DiMNF to suppress *SAA1* expression is consistent with the suppression observed with other functionally diverse AHR ligands (Patel et al., 2009; Murray et al., 2010b,c) and indicates that repression is not ligand-specific. Furthermore, this study demonstrates that repressive SAhRM activity elicited by DiMNF can be extended to additional inflammatory components beyond *SAA1*. C3 expression has been demonstrated to be pivotal in inflammatory diseases, including rheumatoid arthritis, as exemplified by C3(−/−) mouse models, which are resistant to experimentally induced arthritis (Ji et al., 2001). Likewise, the development and severity of experimental autoimmune encephalitis (EAE), a model for multiple sclerosis, has been shown to be dependent on an intact C3-mediated complement system (Szalai et al., 2007). Interestingly, C3(−/+) mice have serum C3 concentrations 50% of their wild-type counterparts and exhibit diminished EAE severity through a mechanism likely to involve reduced migration and activation of T-cells within the spinal cord (Szalai et al., 2007). Here, we reveal that DiMNF, acting as an SAhRM, has the capacity to suppress C3 levels by 40% in vitro, suggesting that DiMNF may be effective therapeutically. However, the efficacy of DiMNF remains to be established with in vivo models, such as EAE. The absence of agonist (i.e., DRE-binding associated with DiMNF) indicates that AHR is not binding to the C3 promoter directly but may tether to a transcriptional complex (e.g., the estrogen receptor, a known inducer of C3 to illicit suppression). Chromatin immunoprecipitation may address such questions and allow the mechanism of suppression to be determined.

This study is the first to identify a flavone-based SAhRM with the capacity to suppress cytokine-mediated inflammatory gene expression in an AHR-dependent manner and indicates that minor modifications of characterized AHR agonists can profoundly influence the direction of AHR activity. Furthermore, the characterization of 3', 4'-dimethoxy- $\alpha$ -naphthoflavone as a SAhRM expands the repertoire of chemical classes that can dissociate the repressive capacity of AHR away from its transactivation function, with the implication that more potent SAhRMs may become evident and used therapeutically as anti-inflammatory agents.

#### Acknowledgments

We acknowledge the generous gift of TCDD by Dr. S. Safe (Texas A&M University, College Station, TX). We are also grateful to Marcia Perdew for editorial assistance in the preparation of this manuscript.

#### Authorship Contributions

*Participated in research design:* Murray, Kolluri, and Perdew.  
*Conducted experiments:* Murray, Flaveny, Tanos, Chiaro, Schroeder, Bisson, and Sharma.  
*Contributed new reagents or analytic tools:* Bisson, Kolluri, Sharma, and Amin.  
*Performed data analysis:* Murray, Flaveny, and Sharma.  
*Wrote or contributed to the writing of the manuscript:* Murray, Bisson, Kolluri, Amin, and Perdew.  
*Other:* Perdew acquired funding for the research.

#### References

Ashida H, Nishiumi S, and Fukuda I (2008) An update on the dietary ligands of the AhR. *Expert Opin Drug Metab Toxicol* 4:1429–1447.  
 Beischlag TV, Luis Morales J, Hollingshead BD, and Perdew GH (2008) The aryl

hydrocarbon receptor complex and the control of gene expression. *Crit Rev Eukaryot Gene Expr* 18:207–250.  
 Bisson WH, Koch DC, O'Donnell EF, Khalil SM, Kerkvliet NI, Tanguay RL, Abagyan R, and Kolluri SK (2009) Modeling of the aryl hydrocarbon receptor (AhR) ligand binding domain and its utility in virtual ligand screening to predict new AhR ligands. *J Med Chem* 52:5635–5641.  
 Boitano AE, Wang J, Romeo R, Bouchez LC, Parker AE, Sutton SE, Walker JR, Flaveny CA, Perdew GH, Denison MS, et al. (2010) Aryl hydrocarbon receptor antagonists promote the expansion of human hematopoietic stem cells. *Science* 329:1345–1348.  
 Cheng N, He R, Tian J, Ye PP, and Ye RD (2008) Cutting edge: TLR2 is a functional receptor for acute-phase serum amyloid A. *J Immunol* 181:22–26.  
 Cho SY, Park SJ, Kwon MJ, Jeong TS, Bok SH, Choi WY, Jeong WI, Ryu SY, Do SH, Lee CS, et al. (2003) Quercetin suppresses proinflammatory cytokines production through MAP kinases and NF-kappaB pathway in lipopolysaccharide-stimulated macrophage. *Mol Cell Biochem* 243:153–160.  
 Ciolano HP, Daschner PJ, and Yeh GC (1999) Dietary flavonols quercetin and kaempferol are ligands of the aryl hydrocarbon receptor that affect CYP1A1 transcription differentially. *Biochem J* 340:715–722.  
 Flaveny CA, Murray IA, Chiaro CR, and Perdew GH (2009) Ligand selectivity and gene regulation by the human aryl hydrocarbon receptor in transgenic mice. *Mol Pharmacol* 75:1412–1420.  
 García-Lafuente A, Guillamón E, Villares A, Rostagno MA, and Martínez JA (2009) Flavonoids as anti-inflammatory agents: implications in cancer and cardiovascular disease. *Inflamm Res* 58:537–552.  
 Gasiewicz TA, Kende AS, Rucci G, Whitney B, and Willey JJ (1996) Analysis of structural requirements for Ah receptor antagonist activity: ellipticines, flavones, and related compounds. *Biochem Pharmacol* 52:1787–1803.  
 Gillner M, Bergman J, Cambillau C, Fernström B, and Gustafsson JA (1985) Interactions of indoles with specific binding sites for 2,3,7,8-tetrachlorodibenzo-p-dioxin in rat liver. *Mol Pharmacol* 28:357–363.  
 Gu YZ, Hogenesch JB, and Bradfield CA (2000) The PAS superfamily: sensors of environmental and developmental signals. *Annu Rev Pharmacol Toxicol* 40:519–561.  
 Henry EC, Kende AS, Rucci G, Tottleben MJ, Willey JJ, Dertinger SD, Pollenz RS, Jones JP, and Gasiewicz TA (1999) Flavone antagonists bind competitively with 2,3,7,8-tetrachlorodibenzo-p-dioxin (TCDD) to the aryl hydrocarbon receptor but inhibit nuclear uptake and transformation. *Mol Pharmacol* 55:716–725.  
 Ji H, Gauguier D, Ohmura K, Gonzalez A, Duchatelle V, Danoy P, Garchon HJ, Degott C, Lathrop M, Benoist C, et al. (2001) Genetic influences on the end-stage effector phase of arthritis. *J Exp Med* 194:321–330.  
 Jux B, Kadow S, and Esser C (2009) Langerhans cell maturation and contact hypersensitivity are impaired in aryl hydrocarbon receptor-null mice. *J Immunol* 182:6709–6717.  
 Kerkvliet NI, Steppan LB, Vorachek W, Oda S, Farrer D, Wong CP, Pham D, and Mourich DV (2009) Activation of aryl hydrocarbon receptor by TCDD prevents diabetes in NOD mice and increases Foxp3+ T cells in pancreatic lymph nodes. *Immunotherapy* 1:539–547.  
 Kuiper GG, Lemmen JG, Carlsson B, Corton JC, Safe SH, van der Saag PT, van der Burg B, and Gustafsson JA (1998) Interaction of estrogenic chemicals and phytoestrogens with estrogen receptor beta. *Endocrinology* 139:4252–4263.  
 Kushner I and Rzewnicki DL (1994) The acute phase response: general aspects. *Baillieres Clin Rheumatol* 8:513–530.  
 Long WP, Pray-Grant M, Tsai JC, and Perdew GH (1998) Protein kinase C activity is required for aryl hydrocarbon receptor pathway-mediated signal transduction. *Mol Pharmacol* 53:691–700.  
 Lu YF, Santostefano M, Cunningham BD, Threadgill MD, and Safe S (1995) Identification of 3'-methoxy-4'-nitroflavone as a pure aryl hydrocarbon (Ah) receptor antagonist and evidence for more than one form of the nuclear Ah receptor in MCF-7 human breast cancer cells. *Arch Biochem Biophys* 316:470–477.  
 Lu YF, Santostefano M, Cunningham BD, Threadgill MD, and Safe S (1996) Substituted flavones as aryl hydrocarbon (Ah) receptor agonists and antagonists. *Biochem Pharmacol* 51:1077–1087.  
 Murray IA, Flaveny CA, DiNatale BC, Chiaro CR, Schroeder JC, Kusnadi A, and Perdew GH (2010a) Antagonism of aryl hydrocarbon receptor signaling by 6,2',4'-trimethoxyflavone. *J Pharmacol Exp Ther* 332:135–144.  
 Murray IA, Krishnegowda G, DiNatale BC, Flaveny C, Chiaro C, Lin JM, Sharma AK, Amin S, and Perdew GH (2010b) Development of a selective modulator of aryl hydrocarbon (Ah) receptor activity that exhibits anti-inflammatory properties. *Chem Res Toxicol* 23:955–966.  
 Murray IA, Morales JL, Flaveny CA, Dinatale BC, Chiaro C, Gowdhalhi K, Amin S, and Perdew GH (2010c) Evidence for ligand-mediated selective modulation of aryl hydrocarbon receptor activity. *Mol Pharmacol* 77:247–254.  
 Pandini A, Soshilov AA, Song Y, Zhao J, Bonati L, and Denison MS (2009) Detection of the TCDD binding-fingerprint within the Ah receptor ligand binding domain by structurally driven mutagenesis and functional analysis. *Biochemistry* 48:5972–5983.  
 Patel RD, Murray IA, Flaveny CA, Kusnadi A, and Perdew GH (2009) Ah receptor represses acute-phase response gene expression without binding to its cognate response element. *Lab Invest* 89:695–707.  
 Petrusis JR and Perdew GH (2002) The role of chaperone proteins in the aryl hydrocarbon receptor core complex. *Chem Biol Interact* 141:25–40.  
 Poland A, Glover E, Ebetino FH, and Kende AS (1986) Photoaffinity labeling of the Ah receptor. *J Biol Chem* 261:6352–6365.  
 Quintana FJ, Basso AS, Iglesias AH, Korn T, Farez MF, Bettelli E, Caccamo M, Oukka M, and Weiner HL (2008) Control of T(reg) and T(H)17 cell differentiation by the aryl hydrocarbon receptor. *Nature* 453:65–71.  
 Savolainen HA and Isomäki HA (1993) Decrease in the number of deaths from secondary amyloidosis in patients with juvenile rheumatoid arthritis. *J Rheumatol* 20:1201–1203.  
 Schäcke H, Schottelius A, Döcke WD, Strehlke P, Jaroch S, Schmees N, Rehwinkel H, Hennekes H, and Asadullah K (2004) Dissociation of transactivation from



- transrepression by a selective glucocorticoid receptor agonist leads to separation of therapeutic effects from side effects. *Proc Natl Acad Sci USA* **101**:227–232.
- Sekine H, Mimura J, Oshima M, Okawa H, Kanno J, Igarashi K, Gonzalez FJ, Ikuta T, Kawajiri K, and Fujii-Kuriyama Y (2009) Hypersensitivity of aryl hydrocarbon receptor-deficient mice to lipopolysaccharide-induced septic shock. *Mol Cell Biol* **29**:6391–6400.
- Singh KP, Casado FL, Opanashuk LA, and Gasiewicz TA (2009) The aryl hydrocarbon receptor has a normal function in the regulation of hematopoietic and other stem/progenitor cell populations. *Biochem Pharmacol* **77**:577–587.
- Steffan RJ, Matelan E, Ashwell MA, Moore WJ, Solvibile WR, Trybulski E, Chadwick CC, Chippari S, Kenney T, Eckert A, et al. (2004) Synthesis and activity of substituted 4-(indazol-3-yl)phenols as pathway-selective estrogen receptor ligands useful in the treatment of rheumatoid arthritis. *J Med Chem* **47**:6435–6438.
- Szalai AJ, Hu X, Adams JE, and Barnum SR (2007) Complement in experimental autoimmune encephalomyelitis revisited: C3 is required for development of maximal disease. *Mol Immunol* **44**:3132–3136.
- Van Dross RT, Hong X, and Pelling JC (2005) Inhibition of TPA-induced cyclooxygenase-2 (COX-2) expression by apigenin through downregulation of Akt signal transduction in human keratinocytes. *Mol Carcinog* **44**:83–91.
- Veldhoen M, Hirota K, Christensen J, O'Garra A, and Stockinger B (2009) Natural agonists for aryl hydrocarbon receptor in culture medium are essential for optimal differentiation of Th17 T cells. *J Exp Med* **206**:43–49.
- Veldhoen M, Hirota K, Westendorf AM, Buer J, Dumoutier L, Renauld JC, and Stockinger B (2008) The aryl hydrocarbon receptor links TH17-cell-mediated autoimmunity to environmental toxins. *Nature* **453**:106–109.
- Zhang S, Lei P, Liu X, Li X, Walker K, Kotha L, Rowlands C, and Safe S (2009) The aryl hydrocarbon receptor as a target for estrogen receptor-negative breast cancer chemotherapy. *Endocr Relat Cancer* **16**:835–844.
- Zhang S, Qin C, and Safe SH (2003) Flavonoids as aryl hydrocarbon receptor agonists/antagonists: effects of structure and cell context. *Environ Health Perspect* **111**:1877–1882.

---

**Address correspondence to:** Dr. Gary H. Perdew, Smith Professor, Center for Molecular Toxicology and Carcinogenesis, Department of Veterinary Sciences, The Pennsylvania State University, 309A Life Sciences Building, University Park, PA 16802. E-mail: ghp2@psu.edu

---